VIP Prodrugs Very Important Paper

International Edition: DOI: 10.1002/anie.201800288
German Edition: DOI: 10.1002/ange.201800288

Bioorthogonal Catalytic Activation of Platinum and Ruthenium Anticancer Complexes by FAD and Flavoproteins

Silvia Alonso-de Castro, Aitziber L. Cortajarena, Fernando López-Gallego, and Luca Salassa**

Abstract: *Recent advances in bioorthogonal catalysis promise to deliver new chemical tools for performing chemoselective transformations in complex biological environments. Herein, we report how FAD (flavin adenine dinucleotide), FMN (flavin mononucleotide), and four flavoproteins act as unconventional photocatalysts capable of converting Pt^{IV} and Ru^{II} complexes into potentially toxic Pt^{II} or Ru^{II}–OH_2 species. In the presence of electron donors and low doses of visible light, the flavoproteins mini singlet oxygen generator (miniSOG) and NADH oxidase (NOX) catalytically activate Pt^{IV} prodrugs with bioorthogonal selectivity. In the presence of NADH, NOX catalyzes Pt^{IV} activation in the dark as well, indicating for the first time that flavoenzymes may contribute to initiating the activity of Pt^{IV} chemotherapeutic agents.*

The latest advances in bioorthogonal chemistry[1] demonstrate how organometallic compounds and inorganic materials are capable of catalyzing the activation of profluorescent substrates and prodrugs with remarkable efficiency in biological environments.[2–10] These selective catalysts carry out non-natural reactions dodging the interference of biological molecules, in some cases with endogenous cellular components as co-reactants.[3,9]

In this context, we recently reported a new bioorthogonal reaction in which riboflavin photoactivates a Pt^{IV} prodrug in a catalytic process under irradiation with extremely low doses of blue light and in the presence of zwitterionic electron donors. Light activation of the riboflavin–prodrug pair triggers cisplatin-related antiproliferative activity in PC3 cancer cells.[11] Unlike in classic organometallic catalysis, where metals act as catalysts, in this reaction, the metal complex is an unconventional substrate,[12] and the biocompatible riboflavin acts as catalyst.

Herein, we report fundamental discoveries in this new area of bioorthogonal chemistry by 1) investigating the catalytic behavior of various flavin catalysts, including four flavoproteins with diverse biological functions and flavin binding pockets, 2) increasing the pool of inorganic reactions to different Pt^{IV} and Ru^{II} prodrug complexes, and 3) evaluating the efficiency of different (bio)organic electron donors (Figure 1). Furthermore, our work shows for the first time that certain flavoproteins may be directly implicated in the activation of metallodrugs under biologically relevant conditions in the absence of light.

Initially, we investigated the capability of FAD (flavin adenine dinucleotide) to act as a catalyst for the photoactivation of two classes of anticancer metal complexes, namely octahedral Pt^{IV} and Ru^{II}–arene piano-stool complexes. Complexes **1**–**3** are prodrugs of cisplatin and carboplatin,[13] and complexes **4** and **5** are photoactivatable scaffolds capable of generating reactive Ru–OH_2 species that can bind to biomacromolecules (Figure 2a).[14–17] Importantly, these Pt^{IV} and Ru^{II} complexes have poor absorption properties in the visible region (Figure 2b) compared to other photoactivatable complexes, such as Ru polypyridyl species. Therefore, novel strategies to prompt their photochemistry at longer wavelengths are pivotal for their use in photochemotherapy. Complexes **1**–**5** are stable towards hydrolysis in the dark, and have either no or poor photoreactivity under blue light excitation.[11,17,18]

FAD photocatalysis towards **1**–**5** was performed employing 10 μM of catalyst and 200 μM of metal substrate (5% catalyst loading). In all irradiation experiments, we used an LED light source (6 mW cm^{-2}) with an emission maximum at 460 nm and ^{1}H NMR analysis to monitor and quantify the evolution of the photoreactions. The experimental methods and a complete set of dark and light-irradiation experiments are described in the Supporting Information (Figures S1–S76).

First, we evaluated the effect of electron donors on the catalytic process using complex **1**, with the aim of optimizing the reaction conditions. Three concentrations (0.2, 2, and 20 mM) of MES (as buffer, pH 6) or NADH in phosphate buffer (PB, pH 7, 100 mM) were employed for this purpose. MES was selected as an electron donor to follow up our previous work on riboflavin[11] while NADH was chosen for its relevance as a biological cofactor in numerous reactions catalyzed by flavoenzymes.[19] Moreover, metal-based cata-

[*] Prof. L. Salassa
Donostia International Physics Center
Paseo Manuel de Lardizabal 4, Donostia, 20018 (Spain)
E-mail: lsalassa@dipc.org
S. Alonso-de Castro, Prof. A. L. Cortajarena, Prof. F. López-Gallego
CIC biomaGUNE
Paseo de Miramón 182, Donostia, 20014 (Spain)
E-mail: flopezgallego@unizar.es
Prof. A. L. Cortajarena, Prof. L. Salassa
Ikerbasque, Basque Foundation for Science
Bilbao, 48011 (Spain)
Prof. F. López-Gallego
ARAID Foundation, Zaragoza (Spain)
Supporting information and the ORCID identification number(s) for the author(s) of this article can be found under: https://doi.org/10.1002/anie.201800288.

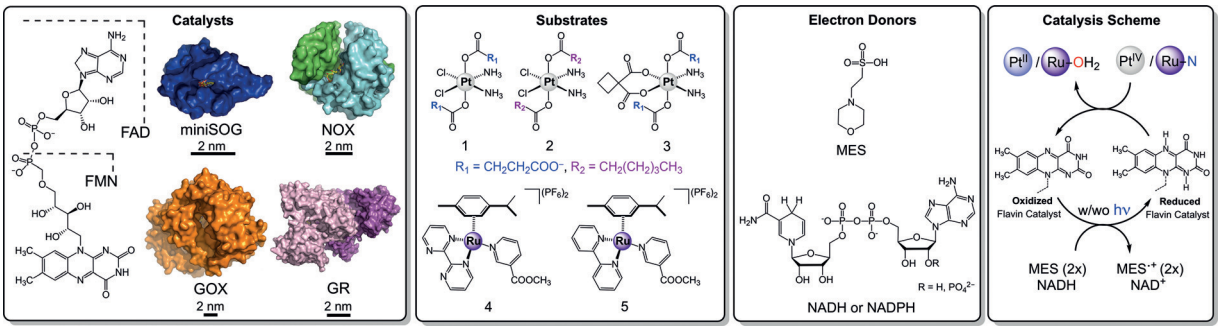

Figure 1. Structures of the catalysts, substrates, and electron donors employed in this study and proposed catalysis mechanism.

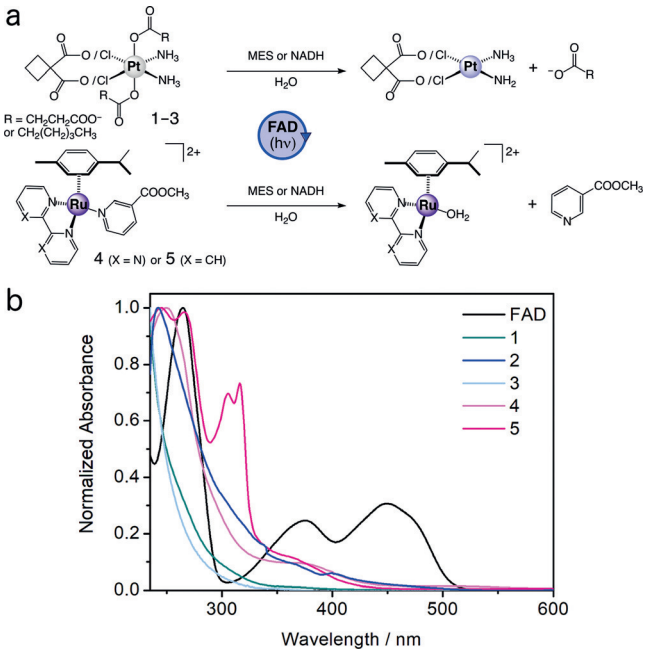

Figure 2. a) Flavin-mediated photoactivation reactions of complexes **1**–**5**. b) Absorption spectra of FAD and **1**–**5**.

lytic drugs have been recently shown to kill cancer cells by interfering with cellular NAD^+/NADH homeostasis.[20–22]

Upon 460 nm light excitation, FAD photoconverted the Pt^{IV} substrate, and the catalytic efficiency increased linearly with the MES concentration. FAD was fully inactive in the dark at any tested MES concentration. In the absence of light, 0.2 or 2 mM NADH did not induce any reaction for **1**, whereas light irradiation switched on the generation of photoproducts at 2 mM NADH when FAD was present. At 2 mM NADH, FAD photocatalyzed the full conversion of **1** in only 2.5 min whereas a reaction time of 5–10 min was required with 20 mM MES. At the lowest concentration (0.2 mM), NADH was instantaneously photooxidized to NAD^+ by molecular oxygen (O_2), precluding any catalytic reaction between FAD and the complex. Conversely, reduction of **1** at 20 mM NADH took place readily in the dark when FAD was present, or under light irradiation when the flavin was absent (Figures S1–S8).

Based on these results, we used 20 mM MES and 2 mM NADH to determine the photocatalytic activity of FAD towards **1**–**5** (Figure 2).[23] All complexes underwent photochemical activation in the presence of catalytic quantities of FAD (Figures S1–S38). In line with their redox chemistry in biological contexts,[24] FAD photoactivation of **1**–**4** with NADH was approximately twice as fast as that with MES. The only exception was **5**, for which the FAD turnover frequency (TOF) was 3.4 times lower with NADH than with MES (Table 1).

Table 1: Turnover frequencies (TOFs, min^{-1}) and total turnover numbers (TTNs) for the FAD- and flavoprotein-catalyzed photoactivation of complexes **1**–**5** in the presence of MES and NADH.

Complex	MES (20 mM)			NADH (2 mM)[a]		
	TOF	TTN	Conv. [%]	TOF	TTN	Conv. [%]
			FAD			
1	2.3 ± 0.2	20	100	5.0 ± 1.7	20	100
2	4.0 ± 0.5	20	100	7.1 ± 1.8	20	100
3	0.6 ± 0.1	11	55	2.3 ± 0.6	14	70
4	4.5 ± 0.6	16	80	9.0 ± 2.3	20	100
5	2.2 ± 0.5	16	80	0.6 ± 0.1	14	70
			miniSOG			
1	1.0 ± 0.2	20	100	7.1 ± 0.4	20	100
2	1.2 ± 0.1	20	100	8.6 ± 2.2	20	100
			NOX			
1	0.62 ± 0.01	20	100	4.3 ± 1.6[b]	20	100
2	4.7 ± 1.2	20	100	8.3 ± 1.6[b]	20	100
			GOX			
1	not active					
2	< 0.1	5	20	< 0.2	7.4	37
			GR[a]			
1	< 0.1	10	50	0.42 ± 0.07	20	100
2	not active			1.2 ± 0.3	20	100

[a] Experiments for GR were run using NADPH. [b] In the dark.

Kinetic analysis of these catalytic reactions showed that the rate clearly depended on the nature of the substrate. Complexes **1**, **2**, and **4** were the best substrates, giving the highest TOFs and total turnover numbers (TTNs). Remarkably, FAD enabled the quantitative conversion of **1** and **2** into the corresponding photoproducts regardless of the electron donor used.

With FAD, a convenient excitation wavelength (460 nm) and an extremely low light dose were employed for the

photoactivation of **1**–**5**. In the case of **1**, **2**, and **4**, a light dose of about 1 J cm^{-2} was sufficient to fully convert the complexes into their activated photoproducts. Ru^{II}–arene derivatives such as **4** and **5** typically require irradiation times exceeding one hour to reach about 50 % conversion (Figures S24 and S32).[14–17] Herein, we show that less than 15 min are sufficient to achieve comparable effects in **4** and **5** when FAD is used as photocatalyst.

In cells, flavins are bound to proteins through covalent and non-covalent interactions,[19] which control their (photo)-redox properties.[24] Exploiting flavoproteins as selective catalysts is therefore an exciting prospect for the design of bioorthogonal activation strategies for metal-based prodrugs. Accordingly, we selected four flavoproteins for their diverse flavin-binding pockets and explored their capacity to catalyze the photoreduction of **1** and **2**. This part of the study was limited to these derivatives for their relevance as anticancer compounds[13,25] with respect to the Ru^{II} complexes **4** and **5**. Furthermore, FAD displayed superior activity towards these Pt^{IV} substrates compared to **3**. The use of **2** was also aimed at gauging the impact of the charge of the substrates on catalysis, with this complex featuring a neutral alkyl chain at the axial position rather than a negatively charged succinate as in **1**.

The flavoprotein catalysts tested were miniSOG (mini singlet oxygen generator),[26] NOX (NADH oxidase from *Thermus thermophilus*),[27] GOX (glucose oxidase from *Aspergillus niger*),[28] and GR (glutathione reductase from *S. cerevisiae*).[29] MiniSOG is a flavin mononucleotide (FMN) containing small protein investigated as a genetically encodable photosensitizer for the selective generation of singlet O_2.[30–32] The bacterial NOX enzyme generates hydrogen peroxide (H_2O_2) from O_2 by oxidizing NADH while the eukaryotic GOX naturally oxidizes glucose to H_2O_2 and D-glucono-δ-lactone. NOX and GOX have both been widely exploited in biocatalysis.[27,33] GR is a NADPH-dependent oxidoreductase exerting a central role in glutathione metabolism for most aerobic organisms.[34] GR was selected because unlike other flavoproteins, it does not generate reactive oxygen metabolites.

Different chemical environments surround the flavin-binding pockets in these four flavoproteins, controlling solvent and substrate accessibility to the active site. As shown in Figure 3, the flavins are more exposed in miniSOG[35] and NOX than in GOX and GR, in which FAD is deeply buried in the protein scaffold. The solvent-accessible surface areas of the flavins are 45.50 Å^2 for miniSOG and 67.92 Å^2 for NOX, but only 2.39 Å^2 for GOX and 4.01 Å^2 for GR. Moreover, they display different electrostatic surfaces in the proximity of the flavin-binding pocket (Figures S39–S43). At pH 6–7, the NOX and GR active sites are neutral, whereas miniSOG and GOX display positive and negative electrostatic charges, respectively.

Unless otherwise stated, photocatalysis experiments (Figures S44–S76) were performed by employing 10 μM of the flavoprotein catalysts, 200 μM of **1** or **2**, and either 20 mM MES or 2 mM NADH to directly compare the activities with that of free flavin under the same conditions. The concentrations of flavins bound to proteins were calibrated by optical methods according to the FAD and FMN (for miniSOG) absorbance at 460 nm. Catalysis results for flavoproteins are summarized in Table 1.

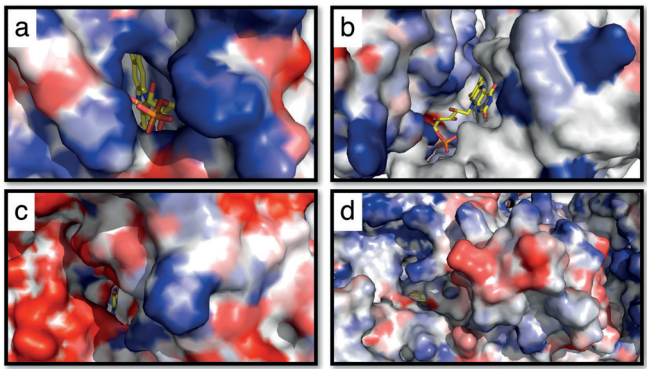

Figure 3. Electrostatic surface potentials of the binding sites of a) miniSOG, b) NOX, c) GOX, and d) GR (calculated using Bluues server). Anionic and cationic residues are shown in red and blue, respectively.[36]

As anticipated from inspecting their flavin active sites, GOX and GR showed the lowest catalytic activity towards the Pt^{IV} substrates. GOX presented no catalytic activity towards **1** under all of the experimental conditions tested. There was also no activity when glucose (20 mM), a natural substrate for the enzyme, was employed as a source of electrons instead of MES or NADH. Conversion of **2** by GOX occurred in the presence of both electron donors but the reactions were slow and did not reach completion after 1 h of light irradiation (conversion $< 40\,\%$). With MES, GR was poorly or not active towards **1** and **2**. On the contrary, the use of NADPH led to significantly higher TOF values and complete substrate conversion within a few minutes of light exposure.

With MES, miniSOG and NOX converted **1** and **2** exclusively into their photoproducts upon blue light excitation. Whereas miniSOG showed no preference between the two substrates, NOX was about seven times more reactive towards **2** than towards **1**. Light irradiation also switched on the catalytic activity of miniSOG in PB/NADH. The flavoprotein achieved full conversion of 200 μM **1** and **2** in about 4 min. In the case of **1**, it is approximately five times less efficient than free FMN (TOF = 35.6 ± 4.3 min^{-1}; Figure S50).

To our surprise, NOX behaved differently, activating **1** and **2** in the dark when co-incubated with 2 mM NADH. Under these conditions, 10 μM NOX completely converted **1** in less than 7.5 min while free FAD did not give any reaction with **1** over 3 h (see above). The TOF values of **1** and **2** for NOX were estimated to be 4.3 ± 1.6 min^{-1} and 8.3 ± 1.6 min^{-1}, respectively, using less than 2 μM of the flavoprotein to allow for NMR reaction monitoring.

The discovery of NOX catalytic activity in the dark has broad relevance for understanding the mechanism of action of Pt^{IV} anticancer agents. It is a common assumption that Pt^{IV} complexes are converted into active species by biological molecular reductants, such as glutathione or ascorbic acid, under physiological conditions.[37] Nevertheless, NOX-catalyzed activation of **1** and **2** in the presence of 2 mM NADH is rapid and suggests that flavoproteins can provide alternative and highly efficient activation pathways for metallodrugs.[38]

Considering that the cellular concentration of NADH is in the 0.1–0.2 mM range,[39] we evaluated the capacity of NOX to convert 200 μM **1** in the presence of an equimolar quantity of NADH in PB (Figure S64). NOX naturally uses O_2 as an electron acceptor to generate H_2O_2 in the presence of NADH.[27] At such low concentrations, the enzyme consumed NADH too rapidly, precluding any catalytic conversion of **1**. For this reason, the reaction was studied under N_2 atmosphere. Accordingly, we determined that NOX could activate approximately 33% of **1** in the absence of O_2, revealing that flavoenzymes may indeed turn on Pt drug activity under certain cellular conditions, that is, hypoxia. Although the Pt^{IV} conversion did not reach completion, the concentration of activated **1** should be sufficient to induce cell death in cancer tissues.

At higher concentrations of electron donor in aerated solution, the enzyme reaction pathway is altered by **1**, which effectively competes with O_2 and intercepts electrons from the reduced flavoenzyme. In fact, the activity of NOX increased by a factor of 2.3 while the production of H_2O_2 simultaneously decreased (Figure 4a) when 1 mM **1** was incubated with equimolar NADH. Under these conditions, the enzyme worked faster because it had access to higher concentrations of electron acceptors (**1** and O_2), and produced lower amounts of H_2O_2 because the hydride of NADH ought to be shared between the O_2 and metal complex reduction reactions. Conversely, miniSOG production of H_2O_2 is independent of the presence of **1** (Table S1) as it likely proceeds through photosensitization.[40]

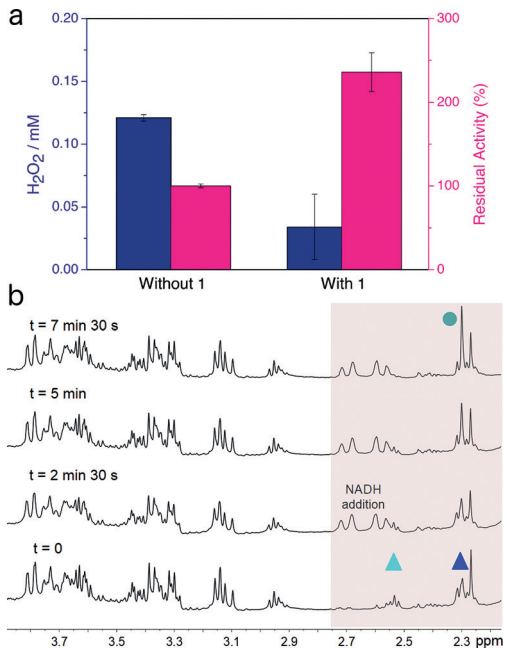

Figure 4. a) Catalytic consumption rate of NADH (magenta) and generation of H_2O_2 (blue) with NOX measured employing a 1:1 ratio of **1** and NADH at a concentration of 1 mM. b) Catalytic activity of NOX in the dark in cell culture medium (pH 7) in the presence of NADH. ^{1}H NMR spectra were recorded for solutions of 200 μM **1** and 10 μM NOX and 2 mM NADH. ^{1}H NMR signal labeling: ▲: Pt–OCO**CH_2**$CH_2CO_2^-$; ▲: Pt–OCOCH_2**CH_2**CO_2^-: ●: free ^-O_2C**CH_2CH_2**CO_2^-.

The capability of miniSOG and NOX to act as bioorthogonal catalysts towards Pt^{IV} prodrugs was investigated by using **1** in cell culture medium, where components such as proteins, vitamins, and salts can interfere with the activation process. Reactions in the presence of NADH (2 mM) showed that miniSOG converted **1** in the biological environment only under light irradiation while the same reaction occurred already in the dark with NOX (Figure 4b and Figure S75). The flavoproteins almost retained the selectivity and efficiency of free FAD under these conditions (Figure S76).

A molecular description of the catalytic mechanism through which free flavins and flavoproteins activate Pt^{IV} and Ru^{II} complexes requires further investigations and is out of the scope of this manuscript. Our previous study suggests the catalysis is linked to the generation of the reduced forms of FAD and FMN (e.g., $FADH_2$ and $FMNH_2$), either through photoinduced electron transfer (MES) or hydride transfer (NADH/NADPH). High levels of electron donors and light help increasing the catalytic efficiency of the flavins by stabilizing their active species and consequently enhancing the reaction rates. Metal complexes may form transient adducts with the reduced flavins and undergo chemical and photochemical transformations.[11]

Nevertheless, it is clear from the results of this study that protein scaffolds play a crucial role in governing the metal substrate access to the flavin catalytic site. Therefore, the negatively charged electrostatic surface of GOX and the shielded channel in which its FAD is bound prevent any interaction with negatively charged **1**. Consistently, we observed that the consumption of glucose by GOX was not affected by the presence of an equimolar amount of **1** (Table S2). Albeit with poor efficiency, GOX activated **2**, which is in agreement with the absence of charged chemical groups in the complex and its lower reduction potential compared to that of **1**.[41]

In the case of miniSOG and NOX, however, the protein scaffold enables the artificial catalysis by facilitating the formation of reduced FMN/FAD and favoring its stabilization for the subsequent electron transfer interaction with the Pt^{IV} substrates. Actually, miniSOG and NOX have more solvent-exposed flavin units and suitable electrostatic surfaces to allow metal substrates to access the active site. The role played by the protein scaffold is dramatic for NOX, which is an enzyme optimized by Nature to transfer hydrides from NADH to electron acceptors. Consistently, NOX activity towards **1** and **2** is observed almost instantaneously in the dark with NADH. On the contrary, miniSOG, a protein derived from phototropin 2, which naturally does not use NADH as a cofactor, requires light activation. Similar to NOX and in contrast to GOX, GR has a mostly neutral FAD binding pocket, which enables the catalytic activation of **1** and **2**. Nonetheless, GR requires light triggering for catalysis likely owing to the limited accessibility of its FAD with respect to NOX.

In conclusion, we have shown that free flavins and flavoproteins can catalyze artificial reactions of Pt^{IV} and Ru^{II} complexes, operating either in the dark or upon light excitation. Some of these unconventional reactions have promising catalytic efficiency and bioorthogonal selectivity.

These findings open new opportunities for the design of chemically and light-activated metal-based prodrugs, whose biological effects could be triggered endogenously by bio-orthogonal flavoprotein catalysts.

Acknowledgements

We thank the Spanish MINECO for grants CTQ2016-80844-R, BIO2016-77367-C2-1-R, BIO2015-69887-R, and BES-2013-065642. COST action CM1303 is also acknowledged for support (F.L.-G.). We also thank the European Research Council (ERC-CoG-648071-ProNANO, A.L.-C.) for support. Dr. D. Padró is acknowledged for his kind support with NMR experiments.

Conflict of interest

The authors declare no conflict of interest.

Keywords: bioorthogonal chemistry · flavoproteins · metal-based prodrugs · photocatalysis · photochemotherapy

How to cite: *Angew. Chem. Int. Ed.* **2018**, *57*, 3143 – 3147
Angew. Chem. **2018**, *130*, 3197 – 3201

[1] J. A. Prescher, C. R. Bertozzi, *Nat. Chem. Biol.* **2005**, *1*, 13 – 21.
[2] P. K. Sasmal, C. N. Streu, E. Meggers, *Chem. Commun.* **2013**, *49*, 1581 – 1587.
[3] T. Völker, F. Dempwolff, P. L. Graumann, E. Meggers, *Angew. Chem. Int. Ed.* **2014**, *53*, 10536 – 10540; *Angew. Chem.* **2014**, *126*, 10705 – 10710.
[4] A. M. Pérez-López, B. Rubio-Ruiz, V. Sebastián, L. Hamilton, C. Adam, T. L. Bray, S. Irusta, P. M. Brennan, G. C. Lloyd-Jones, D. Sieger, J. Santamaría, A. Unciti-Broceta, *Angew. Chem. Int. Ed.* **2017**, *56*, 12548 – 12552; *Angew. Chem.* **2017**, *129*, 12722 – 12726.
[5] J. T. Weiss, J. C. Dawson, K. G. Macleod, W. Rybski, C. Fraser, C. Torres-Sánchez, E. E. Patton, M. Bradley, N. O. Carragher, A. Unciti-Broceta, *Nat. Commun.* **2014**, *5*, 3277.
[6] R. M. Yusop, A. Unciti-Broceta, E. M. V. Johansson, R. M. Sánchez-Martín, M. Bradley, *Nat. Chem.* **2011**, *3*, 239 – 243.
[7] J. Clavadetscher, S. Hoffmann, A. Lilienkampf, L. Mackay, R. M. Yusop, S. A. Rider, J. J. Mullins, M. Bradley, *Angew. Chem. Int. Ed.* **2016**, *55*, 15662 – 15666; *Angew. Chem.* **2016**, *128*, 15891 – 15895.
[8] M. I. Sánchez, C. Penas, M. E. Vázquez, J. L. Mascareñas, *Chem. Sci.* **2014**, *5*, 1901 – 1907.
[9] M. Tomás-Gamasa, M. Martínez-Calvo, J. R. Couceiro, J. L. Mascareñas, *Nat. Commun.* **2016**, *7*, 12538.
[10] G. Y. Tonga, Y. Jeong, B. Duncan, T. Mizuhara, R. Mout, R. Das, S. T. Kim, Y.-C. Yeh, B. Yan, S. Hou, V. M. Rotello, *Nat. Chem.* **2015**, *7*, 597 – 603.
[11] S. Alonso-de Castro, E. Ruggiero, A. Ruiz-de-Angulo, E. Rezabal, J. C. Mareque-Rivas, X. Lopez, F. Lopez-Gallego, L. Salassa, *Chem. Sci.* **2017**, *8*, 4619 – 4625.
[12] L. Gong, Z. Lin, K. Harms, E. Meggers, *Angew. Chem. Int. Ed.* **2010**, *49*, 7955 – 7957; *Angew. Chem.* **2010**, *122*, 8127 – 8129.
[13] T. C. Johnstone, K. Suntharalingam, S. J. Lippard, *Chem. Rev.* **2016**, *116*, 3436 – 3486.
[14] F. Barragán, P. López-Senín, L. Salassa, S. Betanzos-Lara, A. Habtemariam, V. Moreno, P. J. Sadler, V. Marchán, *J. Am. Chem. Soc.* **2011**, *133*, 14098 – 14108.
[15] S. Betanzos-Lara, L. Salassa, A. Habtemariam, O. Novakova, A. M. Pizarro, G. J. Clarkson, B. Liskova, V. Brabec, P. J. Sadler, *Organometallics* **2012**, *31*, 3466 – 3479.
[16] S. Betanzos-Lara, L. Salassa, A. Habtemariam, P. J. Sadler, *Chem. Commun.* **2009**, 6622 – 6624.
[17] A. Habtemariam, C. Garino, E. Ruggiero, S. Alonso-de Castro, C. J. Mareque-Rivas, L. Salassa, *Molecules* **2015**, *20*, 7276 – 7291.
[18] I. Infante, J. M. Azpiroz, N. G. Blanco, E. Ruggiero, J. M. Ugalde, J. C. Mareque-Rivas, L. Salassa, *J. Phys. Chem. C* **2014**, *118*, 8712 – 8721.
[19] D. P. H. M. Heuts, N. S. Scrutton, W. S. McIntire, M. W. Fraaije, *FEBS J.* **2009**, *276*, 3405 – 3427.
[20] R. J. Needham, C. Sanchez-Cano, X. Zhang, I. Romero-Canelón, A. Habtemariam, M. S. Cooper, L. Meszaros, G. J. Clarkson, P. J. Blower, P. J. Sadler, *Angew. Chem. Int. Ed.* **2017**, *56*, 1017 – 1020; *Angew. Chem.* **2017**, *129*, 1037 – 1040.
[21] J. J. Soldevila-Barreda, I. Romero-Canelón, A. Habtemariam, P. J. Sadler, *Nat. Commun.* **2015**, *6*, 6582.
[22] S. Bose, A. H. Ngo, L. H. Do, *J. Am. Chem. Soc.* **2017**, *139*, 8792 – 8795.
[23] After conversion into their aqua complexes, **4** and **5** formed DMSO and NADH adducts in PB buffer (Figures S30 and S38).
[24] S. Weber, E. Schleicher, *Flavins and Flavoproteins*, Springer, New York, **2014**.
[25] S. Dhar, F. X. Gu, R. Langer, O. C. Farokhzad, S. J. Lippard, *Proc. Natl. Acad. Sci. USA* **2008**, *105*, 17356 – 17361.
[26] X. Shu, V. Lev-Ram, T. J. Deerinck, Y. Qi, E. B. Ramko, M. W. Davidson, Y. Jin, M. H. Ellisman, R. Y. Tsien, *PLOS Biol.* **2011**, *9*, e1001041.
[27] J. Rocha-Martín, D. Vega, J. M. Bolivar, C. A. Godoy, A. Hidalgo, J. Berenguer, J. M. Guisán, F. López-Gallego, *BMC Biotechnol.* **2011**, *11*, 101.
[28] V. Leskovac, S. Trivić, G. Wohlfahrt, J. Kandrač, D. Peričin, *Int. J. Biochem. Cell Biol.* **2005**, *37*, 731 – 750.
[29] J. Yu, C.-Z. Zhou, *Proteins Struct. Funct. Bioinf.* **2007**, *68*, 972 – 979.
[30] A. Rodríguez-Pulido, A. L. Cortajarena, J. Torra, R. Ruiz-González, S. Nonell, C. Flors, *Chem. Commun.* **2016**, *52*, 8405 – 8408.
[31] R. Ruiz-González, A. L. Cortajarena, S. H. Mejias, M. Agut, S. Nonell, C. Flors, *J. Am. Chem. Soc.* **2013**, *135*, 9564 – 9567.
[32] M. Westberg, L. Holmegaard, F. M. Pimenta, M. Etzerodt, P. R. Ogilby, *J. Am. Chem. Soc.* **2015**, *137*, 1632 – 1642.
[33] M. D. Gouda, M. S. Thakur, N. G. Karanth, *Biotechnol. Tech.* **1997**, *11*, 653 – 655.
[34] M. Deponte, *Biochim. Biophys. Acta Gen. Subj.* **2013**, *1830*, 3217 – 3266.
[35] Information on the miniSOG structural model is provided in the Experimental Section of the Supporting Information.
[36] I. Walsh, G. Minervini, A. Corazza, G. Esposito, S. C. E. Tosatto, F. Fogolari, *Bioinformatics* **2012**, *28*, 2189 – 2190.
[37] E. Wexselblatt, D. Gibson, *J. Inorg. Biochem.* **2012**, *117*, 220 – 229.
[38] A. Nemirovski, Y. Kasherman, Y. Tzaraf, D. Gibson, *J. Med. Chem.* **2007**, *50*, 5554 – 5556.
[39] N. Ma, M. A. Digman, L. Malacrida, E. Gratton, *Biomed. Opt. Express* **2016**, *7*, 2441 – 2452.
[40] F. M. Pimenta, R. L. Jensen, T. Breitenbach, M. Etzerodt, P. R. Ogilby, *Photochem. Photobiol.* **2013**, *89*, 1116 – 1126.
[41] P. Gramatica, E. Papa, M. Luini, E. Monti, M. B. Gariboldi, M. Ravera, E. Gabano, L. Gaviglio, D. Osella, *J. Biol. Inorg. Chem.* **2010**, *15*, 1157 – 1169.

Manuscript received: January 8, 2018
Accepted manuscript online: January 23, 2018
Version of record online: February 15, 2018

